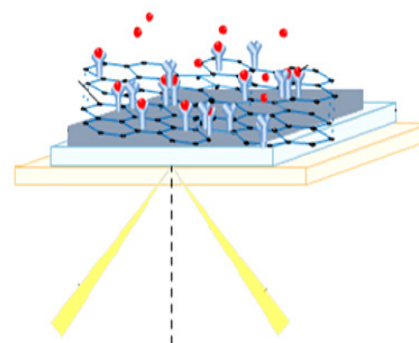




# High sensitivity SPR sensor for liquid phase sample with Ag/PbS/Graphene hybrid nanostructure

Kexiu Dong<sup>1</sup>, Yanping Ji<sup>2</sup>, Jiajia Mi<sup>2</sup>, Xiaotong Zhao<sup>2</sup>,  
Bin Wu<sup>2</sup>, Wangxia Huang<sup>2</sup> and Jianping Shi<sup>2\*</sup>

<sup>1</sup>School of Electronic and Electrical Engineering, Chuzhou University, Chuzhou 239000, China; <sup>2</sup>College of Physics and Electronic Information, Anhui Normal University, Wuhu 241000, China



**Abstract:** A surface plasmon resonance (SPR) sensor with Ag/PbS/GR hybrid nanostructure has been proposed for the diagnostics of liquid phase samples. Here Ag/PbS/GR hybrid nanostructure is designed as an asymmetric MIM waveguide for surface plasmon. Due to the guided wave SPR (GWSPR) modes, the index of the liquid phase samples can be measured more accurately than the conventional SPR sensors. Numerical simulation results show that the sensitivity of the sensor is about 5 times higher than the conventional SPR sensors. The origin of the enhancement mechanism is the combination of GWSPR in the Ag/PbS/GR hybrid nanostructure which enables the surface plasmon to spread along the PbS layer. In Ag/PbS/GR hybrid nanostructure, the electric field is concentrated mostly in the PbS layer, and the enhancement of the field intensity is nearly 30%.

**Keywords:** surface plasmon resonance; surface plasmon waveguide; SPR sensor; sensitivity

**DOI:** 10.3969/j.issn.1003-501X.2017.02.008

**Citation:** *Opto-Elec Eng*, 2017, **44**(2): 198–201

## 1 Introduction

Liquid phase samples, such as protein solution, tissue fluid, and polluted water et al, are very important to human life and health. These samples must be detected with utmost accuracy and therefore the efficient detection mechanism for this kind of samples is significant. Sensors based on surface plasmon resonance (SPR) are widely recognized as valuable tools for sensing liquid phase samples [1-2]. It can be used in real-time monitoring of various biomolecular interactions, such as DNA hybridization and protein bindings [3-4]. It is a simple, direct, real time and sensitive optical sensing technique used for probing refractive index changes.

Different configurations have been proposed for enhancing the sensitivity of sensors based on SPR. In all the configurations, Au and Ag have been used as SPR active metals [5-7]. The major limitation lies in their poor adsorbent of biomolecules, thereby limits the performance of

the biosensor significantly. In recent years, Graphene (GR) has been applied in SPR sensors to improve the sensitivity [8-10]. GR is a single layer of carbon atoms arranged in a two dimensional honeycomb lattice structure with strong bio-molecular affinity. When a solution containing bio-molecules is brought into contact with GR, the binding of biomolecules to the SPR sensor is enhanced, which results in a significant change in refractive index in the vicinity of the sensor surface and hence the sensitivity increases. However the detection sensitivity and accuracy of the sensors are lower for the loss of the electromagnetic field in GR which leads to the damping field and broad resonance peak in the SPR curve.

In this paper, we propose a SPR sensor with Ag/PbS/GR hybrid nanostructure. The Ag/PbS/GR hybrid nanostructure just like a metal-insulator-metal (MIM) waveguide [11-12]. SP is concentrated in the MIM waveguide and enables the enhancement of the evanescent field near the top layer-analyte interface. The enhancement of the evanescent field in such a small area is helpful to enhance the interaction between the SP wave and analyte, and thereby compensates the loss caused by GR. So the sensitivity of the sensor is improved. Moreover, the stability of the sensor is also improved because the nano-layer protect the silver from interacting with the environment.

## 2 Design consideration and theoretical modeling

The proposed configuration with Ag/PbS/GR hybrid nanostructure is shown in Fig.1. It is based on the Kretschmann configuration<sup>[13]</sup> where an Ag nano-membrane is attached to the base of an equilateral prism made of high refractive index glass. On the Ag membrane, a nanoPbS membrane and GR membrane are deposited, respectively. The excitation light wavelength used for the SPR sensing is 700 nm. The TM polarized light is incident from one lateral face of the prism, then reaches its base, and is totally reflected out from the other lateral face, then collects and analyzes by a photodetector.

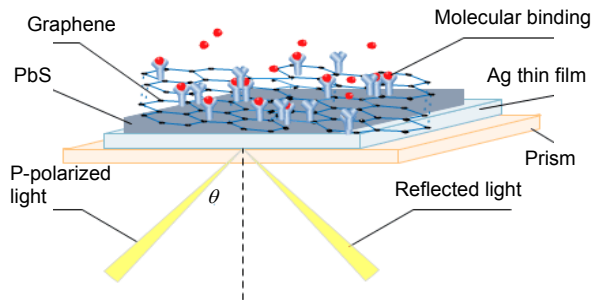


Fig. 1 Schematic diagram of SPR sensor with Ag/PbS/GR hybrid nanostructure.

In this configuration, the matching of propagation constants, known as resonance condition is given as follows<sup>[14]</sup>:

$$n_1 \sin \theta_{\text{SPR}} = \text{Re} \left[ \sqrt{\frac{\epsilon_m n_s^2}{\epsilon_m + n_s^2}} \right], \quad (1)$$

where  $\theta_{\text{SPR}}$  is the angle of incidence at the resonance,  $n_1$  is refractive index of prism,  $\epsilon_m$  is the dielectric constant of metal and  $n_s$  is the effective refractive index of sensing medium and PbS. Because the refractive index of PbS is very high ( $n_{\text{PbS}}=3.92$ ), in order to excite the SPR, we have to choose a larger value of  $n_1$  than the usual configuration. We chose the chalcogenide glass 2S2G as excited prism ( $n_{\text{SG}}=2.33$ ) at 700 nm.

The metal membrane is Ag in our configuration instead of Au in the conventional SPR sensors. In fact Ag has clearer SPR tip leading to the better sensitivity and accuracy, however, it is too susceptible to oxidation and affect the sensor's reliability. In Ag/PbS/GR hybrid nanostructure the Ag membrane can avoid the oxidation and the corruption due to the protection of PbS and GR layers.

For SPPs-based photonic devices, the MIM waveguide is a fundamental structure. Many references have shown that the MIM waveguide is efficient for subwavelength manipulation of light with an acceptable propagation length thanks to the guided wave SPR (GWSPR) modes<sup>[15-17]</sup>. These modes are propagating along the membrane and can be used for sensing of the covered dielectric me-

dium due to the evanescent field. Here the Ag/PbS/GR hybrid nanostructure is designed as an asymmetric MIM waveguide. The permittivity of Ag and GR are  $-20.7323 + 1.3035i$  and  $6.125 + 8.544i$  at 700 nm, respectively.

## 3 Results and discussion

We use the finite difference time domain (FDTD) method<sup>[18]</sup> to calculate the electromagnetic properties of the sensor. The scheme for FDTD numerical computation is shown in Fig. 2. In the  $x$  direction, the perfectly matched layer (PML) is used as the absorption boundary. In the  $y$  direction, it is Bloch boundary condition. The wavelength of incident light is 700 nm, and mesh size is  $\Delta x = \Delta y = 0.05$  nm. The incident angle is scanned with a step of  $0.01^\circ$ . The incident angle versus reflectivity is recorded to show the sensor's performance.

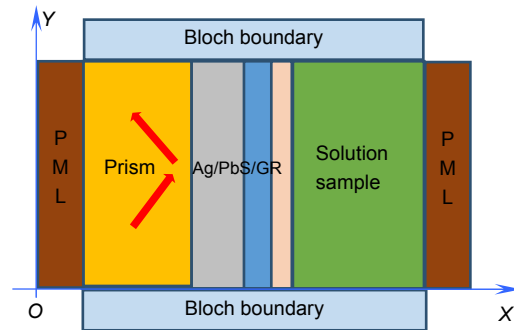


Fig. 2 Schematic for FDTD numerical computation.

The sensitivity of the sensor  $S_n$  is defined as

$$S_n = \frac{\delta \theta_{\text{SPR}}}{\delta n_s}, \quad (2)$$

where  $\delta n_s$  is the change of the refractive index between the standard sample and the test sample,  $\delta \theta_{\text{SPR}}$  is the shift of SPR resonance angle of the test sample relative to the standard sample.

With the sensitivity of the sensor as the target, the structure parameters have been optimized as following: the thickness of Ag and PbS membrane are 50 nm and 17 nm, respectively. The GR is taken one layer with the thickness of 0.34 nm.

We use two sample solutions (DI water and 10% glucose solution) to test the properties of the sensor. DI Water (DIW) is used as the standard sample. The indices of DIW and 10% glucose solution (GS) are 1.330 and 1.338, respectively. SPR characteristics of the sensor depend predominantly on the validity of the resonance condition equation (1) for excitation of plasmons. The most efficient way to check this aspect is to graphically observe the SPR curve, i.e. the curve of incident angle versus reflectivity.

In Fig.3, we give the SPR curves when Ag/PbS/GR hybrid nano-structure is attached to the prism 2S2G. The dash line stands for DIW and the solid line for 10% GS. Obviously there are two resonance peaks at  $67.48^\circ$  and

68.56°, respectively for DIW and 10% GS. The angular shift  $\delta\theta_{PR}$  is found to be 1.08° and the change of the refractive index  $\delta n_s$  is 0.008. So the sensitivity of the sensor is  $S_n=135$  according to formula (2).

For purposes of comparison, we give the SPR curves at the same conditions when only the 50 nm Ag nano membrane is attached to the prism, as shown in Fig.4. The resonance angle are 36.72° and 36.95°, respectively for DIW and 10% GS with an angular shift  $\delta n_s$  of 0.23°. According to formula (2), the sensitivity is 28.75. Clearly the sensitivity of the sensor with Ag/PbS/GR hybrid nanostructure is about 5 times higher than the conventional SPR sensors only based on the Ag nano membrane.

The origin of the enhancement is the combination of the guided wave SPR (GWSPR) in the Ag/PbS/GR hybrid nanostructure which is developed by a MIM nano waveguide and enables the surface plasmons to spread along the dielectric layer PbS. The MIM waveguide is efficient for subwavelength manipulation of light with an acceptable propagation length due to GWSPR modes. Fig.5 shows the electric field distribution in GWSPR mode and non-GWSPR mode. Figs.5(a) and 5(b) are electric field distribution for DIW and 10% GS when incident angles are 67.48° and 68.56° in the proposed sensor corre-

sponding to the GWSPR mode. Figs. 5(c) and 5(d) correspond to the non-GWSPR mode with the incident angles of 36.72° and 36.95° at the same conditions in the conventional sensor.

As can be seen from Figs. 5(a) and 5(b), when the resonance condition (equation (1)) is satisfied, in the sensor with Ag/PbS/GR hybrid nanostructure, the electric field is concentrated mostly in the PbS layer, just like a MIM waveguide. The counterpart to the sensor with only Ag nano-membrane is from 0 nm to 100 nm. Obviously in the proposed sensor, the area of the electromagnetic field is much smaller than that in conventional sensors. This would lead to a huge increment of the field energy per unit area which is beneficial for improving the interaction strength between surface plasmon and analyte. Moreover, because most of the field is now in the dielectric layer which is less absorptive than metal, it is expected that the surface plasmon propagates longer distance along the surface thus increasing the sensitivity. In this sense, the sensitivity enhancement achieved here is similar to the long range SPR.

In addition, we notice that the maximum of the E-field intensity is increased in the MIM waveguide. In the GWSPR, the relative intensity is 16 for DIW and is 15 for

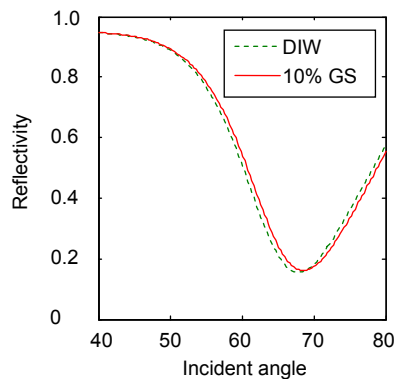


Fig. 3 SPR Curve of Ag/PbS/GR hybrid nano-structure with 2S2G prism for DIW and GS samples.

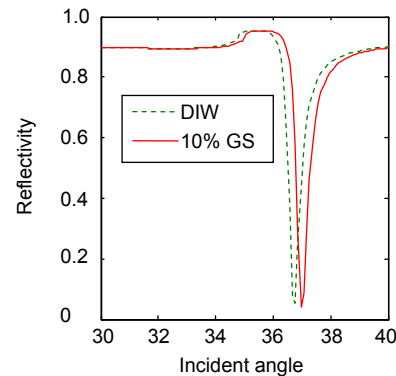


Fig. 4 SPR Curve of 50 nm Ag membrane with 2S2G prism for DIW and GS samples.

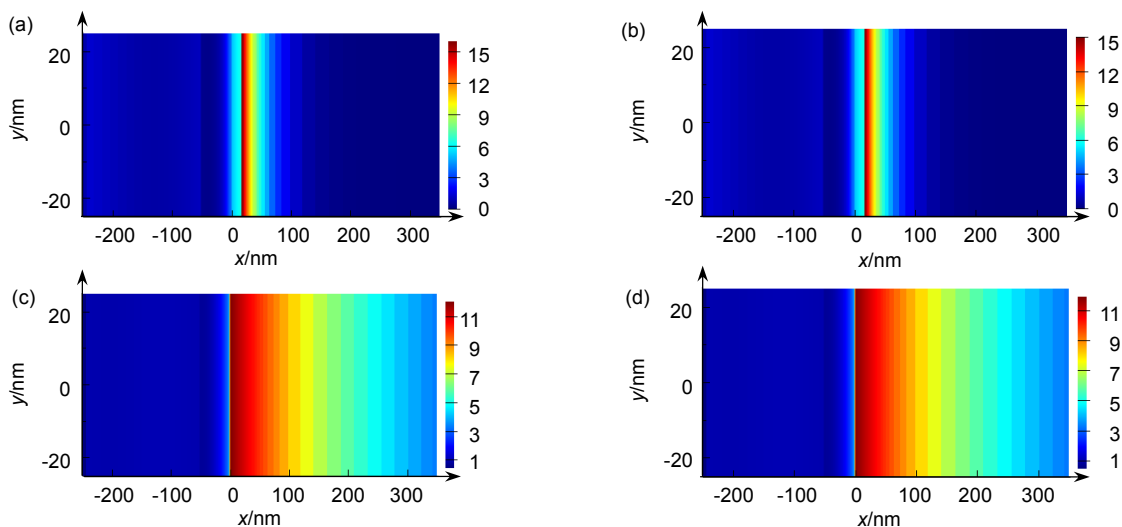


Fig. 5 Electric field distribution in GWSPR mode (a),(b) and non-GWSPR mode (c),(d).

GS, as shown in Figs. 5(a) and 5(b). When there is no GWSPR, the relative intensity drops to about 11 as shown in Figs. 5(c) and 5(d). The enhancement of the field intensity in GWSPR is nearly 30%. It means that in the proposed sensor there is larger intensity and smaller spread size which lead to the higher interactivity between the surface plasmon and samples. In order to display this phenomenon more clearly, we give the cross-section curves of Figs. 4(a) and 4(c) in Fig. 6. As shown in Fig. 6, the maximum of the E-field intensity appears at the interface of prism and Ag ( $x=0$ ) in the traditional sensor. It is different for the sensor with Ag/PbS/GR hybrid nanostructure that the maximum of the E-field intensity is appeared in the waveguide layer ( $x=50$  nm). Moreover, the evanescent field at the sensing interface has been shown clearly. The attenuation distance is about 20 nm and 180 nm for these two sensors respectively that also demonstrate the concentration characteristics of the field in the Ag/PbS/GR hybrid nanostructure.

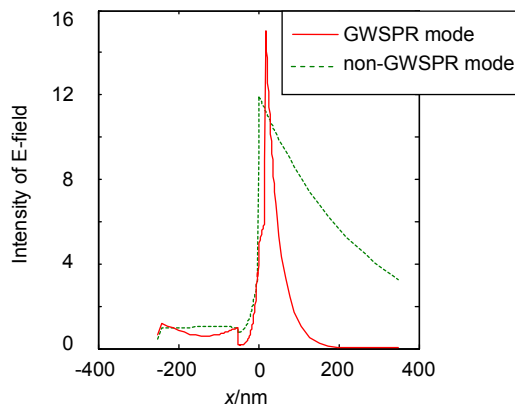


Fig. 6 Cross-section curves of Figs. 4(a) and 4(c).

## 4 Conclusions

We have discussed the SPR sensor with Ag/PbS/Graphene hybrid nanostructure theoretically based on FDTD algorithm. The results show a possibility to reach about 5 times sensitivity as much as the SPR sensor only with Ag nano-membrane. This phenomenon is explained as a result of the combination of the guided wave SPR (GWSPR) in the Ag/PbS/GR hybrid nanostructure and the enhancement of the field near the metal-analyte interface. In addition to high sensitivity, the presented sensor is more suitable for the liquid samples because in Ag/PbS/GR hybrid nanostructure, the Ag membrane can avoid the corruption and oxidation due to the protection of PbS and GR layers.

## Acknowledgments

This work was supported by Anhui University Natural Science Research Project, China (KJ2015A153), National Natural Science Foundation of China (11304002).

## References

- 1 Chung J W, Kim S D, Bernhardt R, *et al.* Application of SPR biosensor for medical diagnostics of human hepatitis B virus (hHBV)[J]. *Sensors and Actuators B: Chemical*, 2005, **111**–**112**: 416–422.
- 2 Riedel T, Rodriguez-Emmenegger C, de los Santos Pereira A, *et al.* Diagnosis of epstein-barr virus infection in clinical serum samples by an SPR biosensor assay[J]. *Biosensors and Bioelectronics*, 2014, **55**: 278–284.
- 3 Williams C, Addona T A. The integration of SPR biosensors with mass spectrometry: possible applications for proteome analysis[J]. *Trends in Biotechnology*, 2000, **18**(2): 45–48.
- 4 Hossain M B, Rana M M. Graphene coated high sensitive surface plasmon resonance biosensor for sensing DNA hybridization[J]. *Sensor Letters*, 2015, **14**(2): 145–152.
- 5 Homola J, Yee S S, Gauglitz G. Surface plasmon resonance sensors: review[J]. *Sensors and Actuators B: Chemical*, 1999, **54**(1–2): 3–15.
- 6 Hutter E, Fendler J. Exploitation of localized surface plasmon resonance[J]. *Advanced Materials*, 2004, **16**(19): 1685–1706.
- 7 Sharma A K, Jha R, Gupta B D. Fiber-optic sensors based on surface plasmon resonance: a comprehensive review[J]. *IEEE Sensors Journal*, 2007, **7**(8): 1118–1129.
- 8 Maharana P K, Jha R, Palei S. Sensitivity enhancement by air mediated graphene multilayer based surface plasmon resonance biosensor for near infrared[J]. *Sensors and Actuators B: Chemical*, 2014, **190**: 494–501.
- 9 Zeng Shuwen, Hu Siyi, Xia Jing, *et al.* Graphene–MoS<sub>2</sub> hybrid nanostructures enhanced surface plasmon resonance biosensors[J]. *Sensors and Actuators B: Chemical*, 2015, **207**: 801–810.
- 10 Meshginqalam B, Toloue H, Ahmadi M T, *et al.* Graphene embedded surface plasmon resonance based sensor prediction model[J]. *Optical and Quantum Electronics*, 2016, **48**: 328.
- 11 Pu Mingbo, Yao Na, Hu Chenggang, *et al.* Directional coupler and nonlinear Mach-Zehnder interferometer based on metal-insulator-metal plasmonic waveguide[J]. *Optics Express*, 2010, **18**(20): 21030–21037.
- 12 Sekkat Z, Hayashi S, Nesterenko D V, *et al.* Plasmonic coupled modes in metal-dielectric multilayer structures: Fano resonance and giant field enhancement[J]. *Optics Express*, 2016, **24**(18): 20080–20088.
- 13 Kretschmann E. The determination of the optical constants of metals by excitation of surface plasmons[J]. *Zeitschrift Für Physik A Hadrons and Nuclei*, 1971, **241**(4): 313–324.
- 14 Maier S A. Plasmonics: fundamentals and applications[M]. New York, US: Springer, 2007.
- 15 Lahav A, Auslender M, Abdulhalim I. Sensitivity enhancement of guided-wave surface-plasmon resonance sensors[J]. *Optics Letters*, 2008, **33**(21): 2539–2541.
- 16 Chandran A, Barnard E S, White J S, *et al.* Metal-dielectric-metal surface plasmon-polariton resonators[J]. *Physical Review B*, 2012, **85**(8): 085416.
- 17 Mrabti A, Lévêque G, Akjouj A, *et al.* Elastoplasmonic interaction in metal-insulator-metal localized surface plasmon systems[J]. *Physical Review B*, 2016, **94**(7): 075405.
- 18 Taflove A, Hagness S C. Finite-difference time-domain solutions of Maxwell's equations[M]. Webster J G. Wiley Encyclopedia of Electrical and Electronics Engineering. New York: John Wiley & Sons, Inc., 2016.